# AN OVERVIEW OF THE CONTROL LAYERS IN LIGO 4KM INTERFEROMETERS

**F. Matichard[1,2], D. Martynov[1], B. Shapiro[3], J. Rollins[2], D. Coyne[2]**

**[1] MIT, Cambridge, MA; [2] Caltech, Pasadena, CA; [3] Stanford University, Stanford, CA; [4] LHO, Hanford, WA**

## 1 INTRODUCTION

The LIGO detectors are based on 4km Michelson interferometers designed to sense the stretch of space-time induced by gravitational waves [1]. To achieve the sensitivity necessary to detect these faint waves, the detectors use multiple auxiliary optical systems including Fabry-Perot cavities in the 4 km arms, mode cleaners and recycling cavities, both for the light source entering the interferometers, and for the light carrying the signal on the output side.

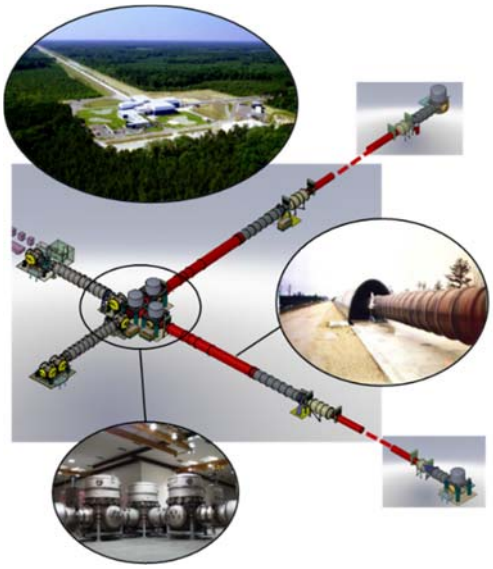

**FIGURE 1: Livingston site and vacuum system**

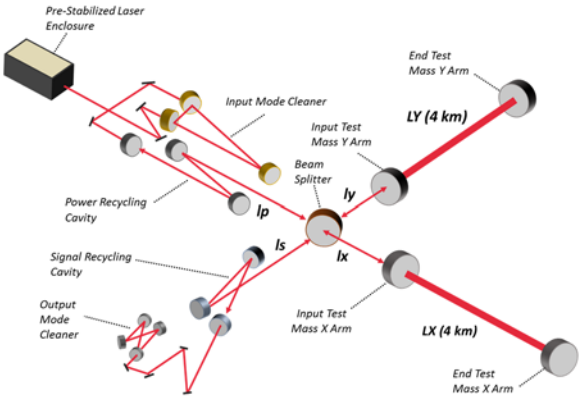


**FIGURE 2: Advanced LIGO simplified optical layout**

FIG. 1 shows a picture of the vacuum envelope which encloses the interferometer at the Livingston site. FIG. 2 shows a simplified optical layout of Advanced LIGO, the new generation of detectors currently operating at the sites [2].

A very high level of vibration isolation is needed to lock the interferometers and cavities on their operating point, and to lower the test masses motion below the amplitude of the gravitational waves. To perform such sensitive measurements twenty active platforms and several tens of passive suspensions are used on each site to isolate the optical components from ground motion. Fig. 3 shows a schematic of the layers of isolation used for the auxiliary optics. Two active platforms are used to provide the low frequency vibration isolation. Suspensions are used to position the optics and provide passive isolation at high frequency.

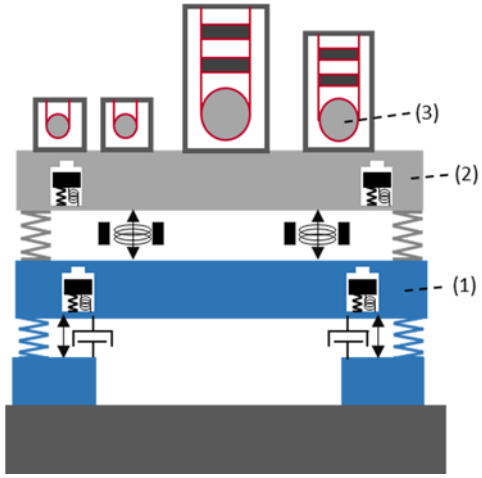


**FIGURE 3: Active platforms (1) & (2), and three-stage suspensions holding the auxiliary optics. Additional layers of isolation are used for the core optics of the interferometer.**

The seismic isolation platforms [3], the suspensions of the optics [4], and the optical cavities [5], are three of the Advanced LIGO sub-systems. They are used in this paper to describe the controls approach used to run this very complex system.

## 2 ACTIVE INERTIAL CONTROL

Active inertial platforms are used to provide the low-frequency vibration isolation. The active inertial concept can be summarized by the schematic in FIG. 4. The motion of the support structure (1) is decoupled from the motion of the

support structure (0) using metal springs (2). Relative motion sensors (3) are used to for the DC positioning and angular control of the platform. Inertial sensors (4) are used for the active vibration isolation in a feedback control scheme. A set of actuators (5) is used to position and isolate the platform in all directions of translation and rotation. Inertial sensors mounted either on the ground or the support structure are used to provide additional isolation in a feedforward control scheme. A detailed presentation of each of the three types of platforms used in Advanced LIGO is given in [3].

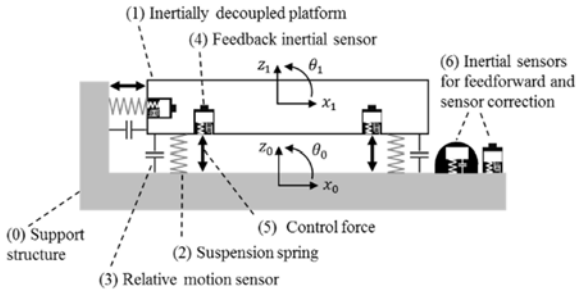


**FIGURE 4: A schematic representation of the active platforms architecture**

The platforms are designed to minimize the cross couplings between the six degrees of freedoms, so that the motion in each direction can be performed using independent controllers. The control approach for one direction is summarized by the block diagram in FIG 5. The input motion disturbance ($X_0$) induces the platform motion ($X_1$) via the seismic path ($P_s$). The platform motion is controlled with the force ($F$) which induces motion via the force path ($P_f$). The feedback block is the central part of the control strategy. The motion of the platform is measured with the inertial sensors which produce the inertial (absolute) motion signal ($U_a$). The signal contains sensor noise ($N_a$). Since inertial sensors sensitivity decreases at low frequency, the signal is filtered with a high-pass ($H$) to avoid sensor noise injection. To complement the control at low frequency, position sensors provide the differential motion signal ($U_r$) between the platform and the input motion. The signal includes sensor noise ($N_r$). This signal is low-pass filtered ($L$) to dominate the control loop at low frequency, and to not compromise the active isolation at high frequency. The combined signal is sent to a compensator ($C_{fb}$) which drives the control force.

Additional isolation is obtained using measurements of the ground motion in a sensor correction scheme at low frequency ($H_{sc}$), and in a feed-forward scheme at high frequency ($C_{ff}$).

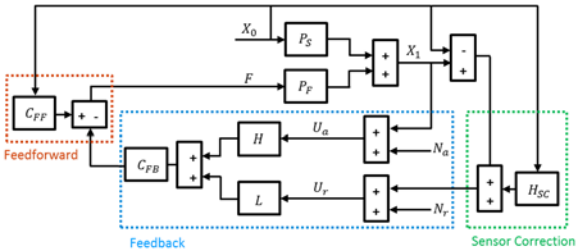


**FIGURE 5: A black diagram representation of the active control scheme**

Further details regarding the control strategy and tuning of the control filters to optimize the performance can be found in [3].

## 3 SUSPENSIONS CONTROL

Passive suspensions are used to position the optics and provide high frequency vibration isolation. Between one and four layers of passive isolation are used depending on the requirements for each optics. This section describes the controls of the most complex of these suspensions: the quadruple pendulum [4].

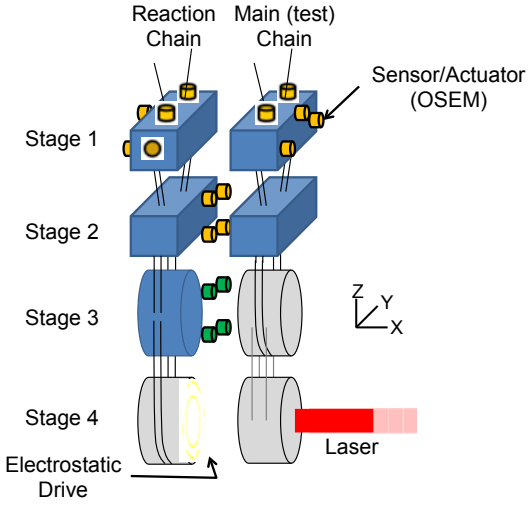


**FIGURE 6: Illustration of the quadruple pendulum**

A detailed description of the control approach can be found in [6], and is summarized in this section. FIG. 6 provides an illustration of the pendulum. It is a stable pendulum consisting of two hanging vertical chains of four stages each. The stages in each chain are numbered top down 1 through 4, where the fourth stage in the main chain is a highly reflective interferometer mirror. The reaction chain is used to provide a quiet actuation platform to filter any disturbance or noise that might couple through the actuators. The chains are about 2 m from top to bottom.

Each stage of the pendulum provides *f*^-2 isolation above the pendulum's resonant frequencies, where *f* represents frequency. Thus,

by using four stages a performance of *f*^-8 is achieved. In this way the pendulum realizes six to seven orders of magnitude of seismic isolation in the single decade between its mechanical resonances and the low frequency end (10 Hz) of LIGO's sensitivity requirement.

There are six collocated sensor/actuator devices called OSEMs (Optical Sensor Electro-Magnet) placed around each stage 1 and referenced to the external frame. These are used to damp the mechanical resonances of the pendulum and provide low frequency mirror positioning control. FIG 7 includes an illustration of this device. The mechanical resonances, between 0.5 Hz and 5 Hz, are purposely designed with very high quality factors to optimize the thermal noise spectrum of the mirror. Damping control is permitted only at stage 1 since the OSEM sensor noise is non-negligible compared to the high sensitivity required. As a result, the pendulum mechanically attenuates the sensor noise through the pendulum chain below. 22 out of 24 modes of vibration for each chain are designed to couple to stage 1 to ensure controllability for the damping loops.

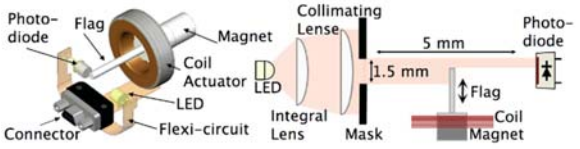


**FIGURE 7: Optical sensor electromagnet [7]**

The position and angular control of the mirror, in addition to low frequency control with the stage 1 actuators, is done with actuators placed between the main and reaction chains at the second, third, and fourth stages. The pendulum is designed to split the mirror control between the various stages so that larger and noisier low frequency control forces are applied to the higher stages where there is better mechanical attenuation to the mirror. The second and third stages have four OSEMs each, and at stage 4 there are four electrostatic actuators known as the Electrostatic Drive (ESD). The error signal sent to each of these stages is the position of only the main chain's stage 4 measured from interferometric signals.

## 4 OPTICAL CAVITIES CONTROL

The four test masses of Advanced LIGO form two arm cavities, as shown in FIG 2. Differential arm length (*Lx-Ly*) is sensitive to gravitational waves while common arm length (Lx+Ly) is used to stabilize the laser frequency. Central part of the detector, known as the dual-recycled Michelson interferometer, consists of the power recycling cavity, the signal recycling cavity and the Michelson interferometer (formed by the beam splitter and the input test masses). The purpose of the power recycling cavity is to increase optical power, resonating in the interferometer, and passively filter laser noises above 0.5 Hz. Michelson interferometer keeps the antisymmetric port near the dark fringe. The signal recycling cavity optimizes the frequency response of the detector.

In order for Advanced LIGO interferometers to be sensitive to gravitational waves, laser light must stably resonate in the optical cavities. This requires stabilization of the longitudinal distances between the optics and their relative alignment [5]. The five degrees of freedoms used to control the interferometers are listed in Table 1.

| | Length | Residual | Error signal | Actuation | Bandwidth |
|---|---|---|---|---|---|
| **Differential arm** | Lx - Ly | 10 fm | DC readout | End test masses | 70 Hz |
| **Common arm** | (Lx + Ly) / 2 | 1 fm | PDH | Laser | 30 kHz |
| **Power recycling** | lp + (lx+ly) / 2 | 1 pm | PDH | Power recycling mirror | 70 Hz |
| **Michelson** | lx-ly | 3 pm | PDH | Beam splitter | 10 Hz |
| **Signal recycling** | ls + (lx+ly) / 2 | 10 pm | PDH | Signal recycling mirror | 20 Hz |

**Table1: Control parameters of Advanced LIGO longitudinal degrees of freedom**

Driven by unsuppressed seismic motion and noise of ISI sensors, mirrors move longitudinally by ~0.3 um and by ~0.1 urad in angle in the frequency range 40 mHz-100 mHz. Motion is significantly less at higher frequencies; but on the time scale of a few hours Advanced LIGO optics can be misaligned by a few urad due to temperature fluctuations.

Operation of Advanced LIGO requires stabilization of relative distance between the test masses on the level of 10 fm and between dual-recycled Michelson optics on the level of 10 pm. Relative alignment fluctuations between the test mass mirrors should be less than 1 nrad. In order to meet these requirements, feedback control system has been developed to transition the interferometer from the free-swinging uncontrolled state to the linear regime [8]. Longitudinal degrees of freedom are controlled using Pound-Drever-Hall (PDH) [9] technique and DC readout [10]. Alignment is maintained using a set of wavefront sensors and quadrant photodetectors. Radio frequency (RF) sidebands at 9 MHz and 45 MHz are introduced for longitudinal and angular controls.

First of all, mirrors are pre-aligned by the procedure known as initial alignment technique. Cavities are

locked one by one and relative alignment between the mirrors is optimized. Then longitudinal stabilization begins. Since all five Advanced LIGO longitudinal degrees of freedom are cross-coupled, two auxiliary lasers are introduced to separate locking of two arm cavities from the central part of the interferometer. Auxiliary lasers are located at the end stations and produce green optical beams with wavelength of 532 nm. These beams resonate in the arm cavities but not in the dual-recycled Michelson interferometer and are extracted through one of the folding power recycling mirrors. The beat between these two beams is used for the differential arm control while the beat between the main laser beam doubled in frequency with one of the end laser beams is used for common arm control as shown in FIG 8.

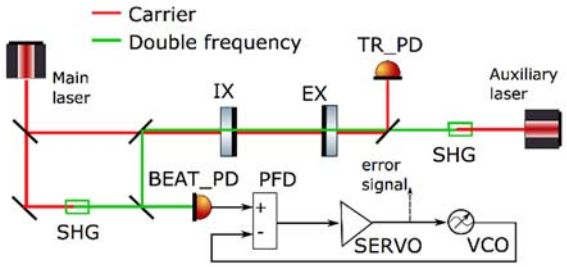


**FIGURE 8: Common arm length stabilization scheme using auxiliary lasers. Frequency of the main and auxiliary lasers is doubled using second harmonic generators (SHG). Auxiliary laser is locked to the arm cavity, consisting of input and end mirrors (IX and EX). Beams from the main laser and the arm cavity beat against each other on the photodetector (BEAT PD). The RF frequency of the voltage controlled oscillator (VCO) is stabilized to the beat note signal. Controls signal to VCO shows the relative frequency difference between the eigen mode of the arm cavity and the main laser. This signal is used as an error signal for the stabilization of the common arm length.**

Common arm is controlled with an offset of 5 nm while dual-recycled Michelson interferometer is locked using PDH signals, derived from the symmetric port of the interferometer. Since PDH error signals, shown in FIG 9, are linear only near the resonance, digital Schmitt trigger is set such that control signal is engaged only when the optical power in the power recycling cavity is above the threshold. If lock is not achieved, control is turned off when optical power falls below a certain threshold.

At this step RF sidebands resonate in the dual-recycled Michelson interferometer, but carrier is still off the resonance in the arm cavities due to the common arm offset. While this offset is slowly removed, optical responses of longitudinal and angular degrees of freedom change. For this reason, error signal of dual-recycled Michelson feedback loops is transitioned to 3Ω PDH signals [11]. These signals are mainly derived from the beat of RF sidebands and are not critically dependent on the carrier light. When common arm offset is reduced to 100 pm, the noise in green beat notes becomes significant for stability and longitudinal control of the differential arm length is transitioned to PDH signal derived from the antisymmetric port. Control of the common arm length is transitioned to DC IR sensors installed in transmission of each arm as shows in FIG 8.

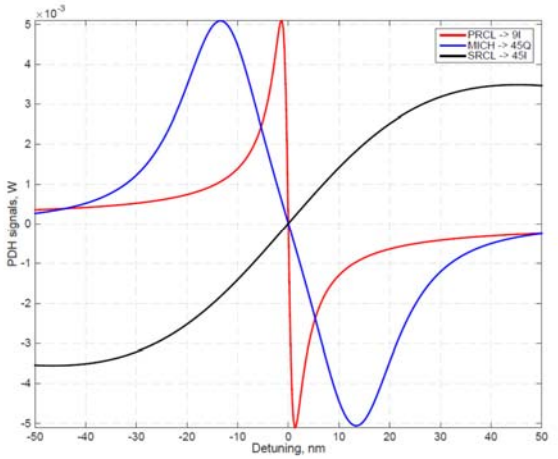


**FIGURE 9: Error signals for power and signal recycling cavity lengths and for Michelson length derived at 9 MHz and 45 MHz at I and Q quadratures.**

Lastly, common arm control is transitioned to low-noise PDH sensor installed at the reflection port, when common arm offset is reduced to 10 pm. Once Advanced LIGO interferometer is in the linear regime, ten angular control servos are engaged in pitch and yaw degrees of freedom to keep relative alignment between the mirrors. Power fluctuations in the arm cavities are stabilized to less than 1% on the time scale of 10 hours. Then differential arm control is transitioned to DC readout and dual-recycled Michelson control is transitioned to 1Ω PDH signals in order to reduce sensing noises.

Dual-recycled Michelson interferometer helps to optimize Advanced LIGO response to gravitational waves. However, feedback control loops of Michelson length and signal recycling cavity length also introduce noise to the differential arm channel due to significant cross couplings. For this reason, online feedforward cancellation technique is employed to subtract longitudinal noise of auxiliary degrees of freedom from the gravitational wave channel.

## 5 ADVANCED CONTROLS

The use of optimization feedback control techniques such as modal, optimal, and adaptive control has been studied and tested at the LIGO test facilities [12]. These studies showed the potential benefits of such approaches. The complexity of these techniques make them, however, difficult to deploy at the observatories, where hundreds of servo-systems are operating in parallel.

Other advanced techniques, related to feedforward optimization have also been studied, and prove to be very effective and easier to deploy at the observatories. They are generally based on the search of coherence between witness sensors and interferometer signals using regression algorithms. The coherent signals are then used to subtract the unwanted noise either in real-time or in the offline data, using algorithms such as the Wiener filtering method [13].

## 6 CONTROLS INFRA-STRUCTURE

The electronics and real-time control system are key components both to achieve low-noise performance and to permit robust operation of complex systems like the Advanced LIGO detectors. Fig 10 (top) gives a schematic overview of a typical electronics diagram for the control of an active module. It uses the active isolation platform as an example. Actual electronics are shown in Fig 11 (bottom). Custom low noise electronics boards and chassis have been designed to condition the instruments signal and to distribute them to the Analog to Digital Converter (ADC), to receive the drive signals from the Digital to Analog Converter (DAC), and then to condition and distribute them to the actuators.

The detailed design is described in [14]. It includes low noise pre-amplification boards designed for the passive geophones [15]. Their design is based on noise budget estimates of the platform motions as described in [16]. Amplification and whitening filter stages are used to maintain the signals above the ADC noise. These stages of amplification can be switched remotely as a function of operating conditions via binary IO cards and relays. The electronics provide read back signals to monitor the state of the switchable filters. The output electronics include anti-image and actuator drivers (valve drivers of hydraulic actuators and coil drivers of electromagnetic actuators). These filtering stages are designed to reduce the DAC noise transmitted to the drivers. Coil drivers voltage and current read backs are sent to the ADC for monitoring.

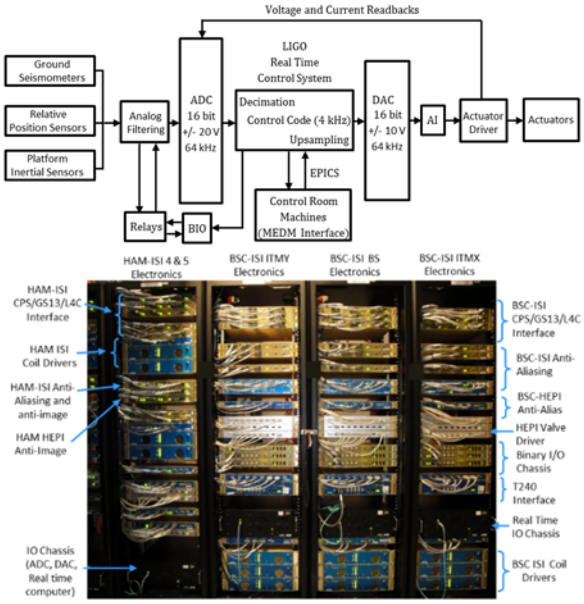


**FIGURE 10: Diagram (a) and actual picture (b) of the isolation systems electronics.**

The signals are digitized at 64 kHz using 16 bits +/- 20V ADC cards. A third order Chebyshev at 10 kHz with a notch at $2^{16}$ Hz is used for the anti-aliasing filter. The signals are decimated to the real time controller sampling frequency (at 2kHz for HEPI platforms, 4 kHz for HAM-ISI and BSC-ISI). The controller output is up-sampled to the DAC cards frequency at 64 kHz. The digital controller is based on the LIGO CDS real time code [17]. An EPICS database [18] is used for communication with the control room machines. The operator interface is built in MEDM code [19].

A software system was developed to coordinate and automate the hierarchical and sequential turn on and turn off process of Advanced LIGO subs-systems (just for the seismic isolation system, each detector uses 21 active platforms, which include up to 12 DOF per platform, several hundreds of parallel feedback and feedforward loops, and thousands of digital channels) [20].

This custom hierarchical state machine, known as Guardian, manages the global state of the interferometers [2]. Written in Python, Guardian consists of a distributed set of automaton nodes, each handling automation for a distinct sub-domain of the instrument. Each node is loaded with a directed state graph that describes the dynamics of its sub-domain. A master manager node at the top of the hierarchy communicates with multiple sub-manager nodes; these in turn communicate with device level nodes at the

bottom of the hierarchy, which directly control the instrument through EPICS. Guardian provides automation of interferometer lock acquisition, as well as the subsequent transitioning to low-noise operation.

## 7 ACKNOWLEDGEMENTS

LIGO was constructed by the California Institute of Technology and Massachusetts Institute of Technology with funding from the National Science Foundation, and operates under cooperative agreement PHY-0757058. Advanced LIGO was built under award PHY-0823459. The material in section 2 on active inertial controls, and in section 6 was previously published in [3], 2015, and is reprinted, with permission of IOP. The material in section 3 on suspension controls was previously published in [6], 2015, and is reprinted, with permission of © IEEE. The material in section 4 was previously presented in Denis Martynov Ph.D thesis [8]. The description of the Guardian in section 6, was previously published in [2], 2015, reprinted with permission from IOP. This paper carries LIGO document number P1600104.

## 8 REFERENCES

1. Abbott, B., et al., *Observation of gravitational waves from a binary black hole merger.* Physical review letters, 2016. **116**(6): p. 061102.

2. Aasi, J., et al., *Advanced LIGO.* Classical and quantum gravity, 2015. **32**(7): p. 074001.

3. Matichard, F., et al., *Seismic isolation of Advanced LIGO: Review of strategy, instrumentation and performance.* Classical and Quantum Gravity, 2015. **32**(18): p. 185003.

4. Aston, S., et al., *Update on quadruple suspension design for advanced LIGO.* Classical and Quantum Gravity, 2012. **29**(23): p. 235004.

5. Staley, A., et al., *Achieving resonance in the Advanced LIGO gravitational-wave interferometer.* Classical and Quantum Gravity, 2014. **31**(24): p. 245010.

6. Shapiro, B., et al., *Selection of important parameters using uncertainty and sensitivity analysis.* Mechatronics, IEEE/ASME Transactions on, 2015. **20**(1): p. 13-23.

7. Carbone, L., et al., *Sensors and actuators for the Advanced LIGO mirror suspensions.* Classical and Quantum Gravity, 2012. **29**(11): p. 115005.

8. Martynov, D.V., *Lock Acquisition and Sensitivity Analysis of Advanced LIGO Interferometers*. 2015, California Institute of Technology.

9. Drever, R., et al., *Laser phase and frequency stabilization using an optical resonator.* Applied Physics B, 1983. **31**(2): p. 97-105.

10. Fricke, T.T., et al., *DC readout experiment in Enhanced LIGO.* Classical and Quantum Gravity, 2012. **29**(6): p. 065005.

11. Arai, K. and T. collaboration, *Sensing and controls for power-recycling of TAMA300.* Classical and Quantum Gravity, 2002. **19**(7): p. 1843.

12. Shapiro, B., N. Mavalvala, and K. Youcef-Toumi. *Modal damping of a quadruple pendulum for advanced gravitational wave detectors*. in *American Control Conference (ACC), 2012*. 2012. IEEE.

13. DeRosa, R., et al., *Global feed-forward vibration isolation in a km scale interferometer.* Classical and Quantum Gravity, 2012. **29**(21): p. 215008.

14. Abbott, B., *SEI Electronics Document Hub, LIGO document T1300173.* 2013.

15. Lantz, B., *LT1012 is the best op-amp for the GS13 preamp, LIGO document T0900457.* 2009.

16. Lantz, B., *Low Frequency motion estimates of the BSC-ISI, LIGO document G050271.* 2005.

17. Bork, R., et al. *New control and data acquisition system in the Advanced LIGO project*. in *Proc. of Industrial Control And Large Experimental Physics Control System (ICALEPSC) conference*. 2011.

18. Dalesio, L.R., et al., *The experimental physics and industrial control system architecture: past, present, and future.* Nuclear Instruments and Methods in Physics Research Section A: Accelerators, Spectrometers, Detectors and Associated Equipment, 1994. **352**(1): p. 179-184.

19. Evans Jr, K., *MEDM Reference Manual.* Argonne National Laboratory, http://www. aps. anl. gov/epics/EpicsDocumentation/ExtensionsManuals/MEDM/MEDM. html, 2006.

20. Rollins, J.G., *Advanced LIGO Automation with Guardian.* LIGO Document G1500506.